Electronic Supplementary Information – Defect formation and ambivalent effects on electrochemical performance in layered sodium titanate $Na_2Ti_3O_7$

Yong-Chol Pak, Chung-Hyok Rim, Suk-Gyong Hwang, Kum-Chol Ri, Chol-Jun Yu*

Chair of Computational Materials Design (CMD), Faculty of Materials Science, Kim Il Sung University, Pyongyang, PO Box 76, Democratic People's Republic of Korea

Table S1. Lattice constants (a, b, c) and lattice angle (β, $\alpha = \gamma = 90°$), unit cell volume (Vol) and band gap (E_g) with each relative error (err) for $Na_2Ti_3O_7$ unit cell, according the value of Hubbard parameter U with PBE+vdW functional and different XC functional of PBEsol with and without vdW.

XC	U (eV)	a (Å)	err (%)	b (Å)	err (%)	c (Å)	err (%)	β (deg)	err (%)	Vol (Å^3)	err (%)	E_g (eV)	ΔE (eV)
PBE+	0.0	9.1227	-0.04	3.7876	-0.32	8.5389	-0.29	101.944	0.34	288.6634	-0.90	3.15	-0.58
vdW	0.5	9.1277	0.02	3.7944	-0.14	8.5416	-0.25	101.925	0.33	289.4444	-0.63	3.19	-0.54
	1.0	9.1336	0.08	3.8015	0.05	8.5440	-0.23	101.915	0.32	290.6667	-0.21	3.24	-0.49
	1.5	9.1397	0.15	3.8087	0.24	8.5462	-0.20	101.905	0.31	291.0952	-0.07	3.29	-0.44
	2.0	9.1469	0.23	3.8160	0.43	8.5479	-0.18	101.896	0.30	291.9525	0.23	3.34	-0.39
	2.2	9.1483	0.24	3.8191	0.51	8.5496	-0.16	101.890	0.29	292.3012	0.35	3.35	-0.38
	2.4	9.1510	0.27	3.8221	0.59	8.5506	-0.15	101.885	0.29	292.6576	0.47	3.37	-0.36
	2.6	9.1537	0.30	3.8252	0.67	8.5519	-0.13	101.881	0.28	293.024	0.60	3.39	-0.34
	2.8	9.1571	0.34	3.8268	0.71	8.5563	-0.08	101.868	0.27	293.4245	0.73	3.44	-0.29
	3.0	9.1598	0.37	3.8297	0.79	8.5573	-0.07	101.871	0.27	293.7643	0.85	3.46	-0.27
	3.2	9.1627	0.40	3.8328	0.87	8.5589	-0.05	101.864	0.27	294.1534	0.98	3.48	-0.25
	3.4	9.1655	0.43	3.8359	0.95	8.5600	-0.04	101.861	0.26	294.5247	1.11	3.50	-0.23
	3.6	9.1686	0.47	3.8390	1.03	8.5607	-0.03	101.853	0.26	294.8980	1.24	3.52	-0.21
	3.8	9.1717	0.50	3.8421	1.12	8.5620	-0.02	101.848	0.25	295.2843	1.37	3.54	-0.19
	4.0	9.1748	0.53	3.8453	1.20	8.5633	0.00	101.843	0.25	295.6789	1.51	3.56	-0.17
PBE	3.0	9.2754	1.64	3.8503	1.33	8.6837	1.40	101.685	0.09	303.6946	4.26	3.39	-0.34
PBEsol	3.0	9.1521	0.29	3.8227	0.61	8.5855	0.26	101.740	0.14	294.0872	0.96	3.42	-0.31
PBEsol+ vdW	3.0	9.0453	-0.88	3.8004	0.02	8.4695	-1.10	101.891	0.29	284.8992	-2.19	3.49	-0.24
Exp.[a]		9.1260		3.7997		8.5634		101.593				3.73	
Exp.[b]		9.1281		3.8022		8.5625		101.603		291.29		3.51	

[a]Ref. [1]
[b]Ref. [2]

Table S2. Pseudopotential file name, valence electron configuration and total energy of isolated atoms, phase, total energy of elementary substances, and binding energy per atom. $E_{\text{bind}} = (E_{\text{tot}}^{\text{sub}} - NE_{\text{tot}}^{\text{atom}})/N$, where N is the number of atoms included in the elementary substance. Values in parenthesis are experimental ones [3].

Element	Pseudopotential	Configuration	$E_{\text{tot}}^{\text{atom}}$ (Ry)	Phase	$E_{\text{tot}}^{\text{sub}}$ (Ry)	E_{bind} (eV/atom)
H	H.pbe-van_ak.UPF	$1s^1$	-0.91703472	gas	-2.33054856	-3.3775
O	O.pbe-van_ak.UPF	$2s^2 2p^4$	-31.55407991	gas	-63.85222829	-5.0618 (-5.12)
Li	Li.pbe-s-van_ak.UPF	$1s^2 2s^{0.95} 2p^{0.05}$	-14.57961031	bcc	-29.44901619	-1.9715
Na	Na.pbe-sp-van_ak.UPF	$2s^2 2p^6 3s^1$	-96.04691566	bcc	-192.30620110	-1.4447
K	K.pbe-sp-van.UPF	$3s^2 3p^6 4s^1$	-57.13828878	bcc	-114.42571753	-1.0146
Rb	rb_pbe_v1.uspp.F.UPF	$4s^2 4p^6 5s^{0.5}$	-53.09506539	bcc	-106.32626483	-0.9261
Ti	Ti.pbe-sp-van_ak.UPF	$3s^2 3p^6 4s^2 3d^2$	-116.21833062	hcp	-349.47942556	-3.7390

*Corresponding author: Chol-Jun Yu, Email: cj.yu@ryongnamsan.edu.kp

Table S3. Crystal system, space group, total energy, and formation energy per O_2 of binary metal oxides. $E_{\rm form}(M_aO_b) = [E_{\rm tot}(M_aO_b) - aE_{\rm tot}(M) - b/2E_{\rm tot}(O_2)] \cdot 2/b$, where $E_{\rm tot}(M)$ is the total energy of elementary metal per atom and $E_{\rm tot}(O_2)$ is the total energy of isolated O_2 molecule. Experimental values are from Ref. [4].

				$E_{\rm form}$ (eV/O_2)	
Compound	Structure	Space group	$E_{\rm tot}$ (Ry)	Cal.	Exp.
Superoxide					
LiO_2	cubic	$Fm\bar{3}m$	-314.48820427	-0.6165	–
NaO_2	cubic	$Fm\bar{3}m$	-640.88614287	-2.9417	
	orthorhombic	$Pnnm$	-320.46159754	-3.0677	
	cubic	$Pa\bar{3}$	-640.90653854	-3.0110	
	hexagonal	$R\bar{3}m$	-480.64680752	-2.8609	-2.6950
KO_2		$C12c1$	-485.13970635	-2.9911	
		$F4mmm$	-485.24565685	-3.3515	
		$I4mmm$	-242.62272452	-3.3508	-2.9508
RbO_2	cubic	$Fm\bar{3}m$	-233.89551457	0.9198	
		$I4mmm$	-234.52715354	-3.3772	-2.8866
Peroxide					
Li_2O_2	hexagonal	$P6_3/mmc$	-187.60021477	-6.7874	-6.5697
Na_2O_2	hexagonal	$P62m$	-769.65319364	-5.3421	-5.2916
K_2O_2		$Cmca$	-714.65068764	-5.2345	-5.1176
Rb_2O_2		$Immm$	-341.12271964	-5.2092	-4.8887
Oxide					
Li_2O	cubic	$Fm\bar{3}m$	-247.43533953	-13.1624	
	hexagonal	$R3\bar{m}h$	-185.57950678	-13.1896	-12.3854
Na_2O	cubic	$Fm\bar{3}m$	-898.28499053	-9.2229	-8.5801
K_2O	cubic	$Fm\bar{3}m$	-586.55663718	-7.8187	-7.4884
Rb_2O	cubic	$Fm\bar{3}m$	-554.11294202	-7.5065	-7.0224
TiO	cubic	$Fm\bar{3}m$	-595.0146926	-9.1000	
	monoclinic	$C2/m$	-743.8754339	-9.6827	
			-743.8779393	-9.6964	-10.7655
TiO_2	monoclinic	$C2/m$	-724.0974288	-9.2382	
	tetragonal	$I4_1/amd$	-362.0508892	-9.2530	
	monoclinic	$P2_1/c$	-724.0739579	-9.1583	
	tetragonal	$P4_2/mnm$	-362.0443419	-9.2084	
	orthorhombic	$Pbca$	-1448.2300363	-9.2980	
	orthorhombic	$Pbcn$	-724.1290851	-9.3458	-9.7774
Ti_2O_3	hexagonal	$R\bar{3}c$	-659.7025193	-9.8563	-10.5018
Ti_3O_5	monoclinic	$C2/c$	-1021.8435757	-9.8604	
	monoclinic	$C2/m$	-1021.7055992	-9.4849	
	orthorhombic	$Cmcm$	-1021.6864610	-9.4328	-10.1892

Table S4. Crystal system with space group, total energy, and formation energy of sodium oxides calculated using oxygen gas and sodium metal as two end materials, and corrected formation energy. $E_{\rm form} = \frac{1}{a+b}E_{\rm tot}(M_aO_b) - [xE_{\rm tot}(M) - (1-x)E_{\rm tot}(O_2)/2]$, where $x = a/(a+b)$. The correcting term $E_{\rm corr}$ is determined from $E^0_{\rm corr}$ shown in Fig. S1 by using the relation $E_{\rm corr} = E^0_{\rm corr}(1-x)/2$, and then, the corrected formation energy is obtained by $E^{\rm corr}_{\rm form} = E_{\rm form} - E_{\rm corr}$.

M_aO_b	phase	a	b	$x = a/(a+b)$	$E_{\rm tot}(M_aO_b)$ (Ry)	$E_{\rm form}$ (eV)	$E_{\rm corr}$ (eV)	$E^{\rm corr}_{\rm form}$ (eV)
O_2	gas	0	2	0.0	-63.85222829	0.0000		0.0000
NaO_3	orthorhombic ($Imm2$)	1	3	1/4	-192.122132689	-0.6486		-0.6486
NaO_2	cubic ($Fm\bar{3}m$)	1	2	1/3	-160.221535717	-0.9806	-0.1404	-0.8401
	orthorhombic ($Pnnm$)				-160.236595150	-1.0489		-0.9084
	cubic ($Pā3$)				-160.215602507	-0.9537		-0.8132
	hexagonal ($R\bar{3}m$)				-160.230798769	-1.0226		-0.8822
Na_2O_2	hexagonal ($P\bar{6}2m$)	2	2	1/2	-256.551064545	-1.3355	-0.0441	-1.2914
Na_2O	cubic ($Fm\bar{3}m$)	2	1	2/3	-224.571247632	-1.5372	-0.0942	-1.4429
Na	cubic (bcc)	1	0	1.0	-96.153100550	0.0000		0.0000

Table S5. Crystal system with space group, total energy, and formation energy of titanium oxides calculated using oxygen gas and titanium metal as two end materials. $E_{\text{form}} = \frac{1}{a+b}E_{\text{tot}}(\text{M}_a\text{O}_b) - [xE_{\text{tot}}(\text{M}) - (1-x)E_{\text{tot}}(\text{O}_2)/2]$, where $x = a/(a+b)$.

M_aO_b	phase	a	b	$x = a/(a+b)$	$E_{\text{tot}}(\text{M}_a\text{O}_b)$ (Ry)	E_{form} (eV)
O_2	gas	0	2	0.0	-63.85222547	0.0000
TiO_2	monoclinic ($C2/m$)	1	2	0.3333	-181.02435720	-3.2039
	tetragonal ($I4_1/amd$)				-181.02544461	-3.2088
	monoclinic ($P2_1/c$)				-181.01848948	-3.1773
	tetragonal ($P4_2/mnm$)				-181.02217096	-3.1940
	orthorhombic ($Pbca$)				-181.02875453	-3.2238
	orthorhombic ($Pbcn$)				-181.03227127	-3.2398
Ti_9O_{17}	triclinic ($P\bar{1}$)	9	17	0.3462	-1597.07044234	-3.2106
Ti_8O_{15}	triclinic ($P\bar{1}$)	8	15	0.3478	-1416.03700819	-3.2061
Ti_7O_{13}	triclinic ($P\bar{1}$)	7	13	0.3500	-1235.00172357	-3.1990
Ti_6O_{11}	monoclinic ($C2/m$)	6	11	0.3529	-1053.94010619	-3.1683
Ti_5O_9	triclinic ($P\bar{1}$)	5	9	0.3571	-872.93708920	-3.1814
	triclinic ($P\bar{1}$)	10	18		-1745.91065854	-3.1992
Ti_4O_7	triclinic ($P\bar{1}$)	4	7	0.3636	-691.89925787	-3.1586
Ti_3O_5	monoclinic ($C2/c$)	3	5	0.3750	-510.92178785	-3.2214
	monoclinic ($C2/m$)				-510.85279962	-3.1041
	orthorhombic ($Cmcm$)				-510.84323050	-3.0878
Ti_2O_3	hexagonal ($R\bar{3}c$)	2	3	0.4000	-329.85125963	-3.1063
TiO	monoclinic ($C2/m$)	5	5	0.5000	-743.87793933	-2.6108
	monoclinic ($C2/m$)	1	1	0.5000	-148.77508678	-2.6074
	cubic ($Fm\bar{3}m$)	1	1	0.5000	-148.75367315	-2.4617
Ti_2O	hexagonal ($P\bar{3}m1$)	2	1	0.6667	-265.22033661	-1.6456
Ti_3O	hexagonal ($P312$)	3	1	0.7500	-381.70674692	-1.3046
	hexagonal ($P\bar{3}1c$)				-381.70724216	-1.3063
Ti_6O	hexagonal ($P\bar{3}1m$)	6	1	0.8571	-731.07077997	-0.6813
Ti	hexagonal (hcp)	1	0	1.0	-116.46569363	0.0000

Table S6. Oxygen chemical potential $\Delta\mu_{\text{O}}\,(T, p)$ as increasing temperature T from 300 K to 1500 K with the experimental data of entropy S°, enthalpy difference $H^\circ(T) - H^\circ(Tr)$, and $H^\circ(Tr) - H^\circ(0) = 0.0899$ eV available from Ref. [4], where the reference temperature is $Tr = 298.15$ K. Here, $\Delta\mu_{\text{O}}\,(T, p)$ is evaluated at the pressure values of $p = p_\circ = 1$ atm and $p = 0.2$ atm, respectively.

T		S°	$H^\circ(T) - H^\circ(Tr)$	TS°	$\Delta\mu_{\text{O}}\,(T, p_\circ)$		$k_{\text{B}}T$	$\frac{1}{2}k_{\text{B}}T\ln(p/p_\circ)$	$\Delta\mu_{\text{O}}\,(T, p)$
(°C)	(K)	(J/mol·K)	(kJ/mol)	(kJ/mol)	(kJ/mol)	(eV)	(eV)	(eV)	(eV)
25	298.15	205.148	0.000	61.1649	−26.2424	−0.2718	0.0257	−0.0207	−0.2925
26.85	300	205.330	0.054	61.5990	−26.4325	−0.2738	0.0259	−0.0208	−0.2946
126.85	400	213.873	3.026	85.5492	−36.9216	−0.3824	0.0345	−0.0277	−0.4102
226.85	500	220.695	6.085	110.3475	−47.7913	−0.4950	0.0431	−0.0347	−0.5297
326.85	600	226.454	9.245	135.8724	−58.9737	−0.6108	0.0517	−0.0416	−0.6524
426.85	700	231.470	12.500	162.0290	−70.4245	−0.7294	0.0603	−0.0485	−0.7780
526.85	800	235.925	15.838	188.7400	−82.1110	−0.8505	0.0689	−0.0555	−0.9059
626.85	900	239.937	19.244	215.9433	−94.0097	−0.9737	0.0776	−0.0624	−1.0361
726.85	1000	243.585	22.707	243.5850	−106.0990	−1.0989	0.0862	−0.0693	−1.1683
826.85	1100	246.930	26.217	271.6230	−118.3630	−1.2259	0.0948	−0.0763	−1.3022
926.85	1200	250.019	29.768	300.0228	−130.7874	−1.3546	0.1034	−0.0832	−1.4378
1026.85	1300	252.888	33.352	328.7544	−143.3612	−1.4849	0.1120	−0.0901	−1.5750
1126.85	1400	255.568	36.968	357.7952	−156.0736	−1.6165	0.1206	−0.0971	−1.7136
1226.85	1500	258.081	40.611	387.1215	−168.9153	−1.7495	0.1293	−0.1040	−1.8536

Table S7. Oxygen chemical potential $\Delta\mu_O\,(T, p)$ as decreasing oxygen partial pressure p from 10^{10} atm to 10^{-20} atm at temperatures of T = 1100 K and 700 K, respectively.

p		$\frac{1}{2}k_B T \ln(p/p_\circ)$	$\Delta\mu_O\,(T, p)$	
			T = 1100 K	700 K
(Pa)	(atm)	(eV)	(eV)	(eV)
10^{15}	10^{10}	1.0913	−0.1346	0.3619
10^{12}	10^{7}	0.7639	−0.4620	0.0345
10^{9}	10^{4}	0.4365	−0.7894	−0.2929
10^{6}	10^{1}	0.1091	−1.1168	−0.6203
10^{3}	10^{-2}	−0.2183	−1.4442	−0.9477
10^{0}	10^{-5}	−0.5457	−1.7716	−1.2751
10^{-3}	10^{-8}	−0.8731	−2.0990	−1.6025
10^{-6}	10^{-11}	−1.2005	−2.4264	−1.9299
10^{-9}	10^{-14}	−1.5278	−2.7538	−2.2573
10^{-12}	10^{-17}	−1.8552	−3.0812	−2.5847
10^{-15}	10^{-20}	−2.1826	−3.4086	−2.9121

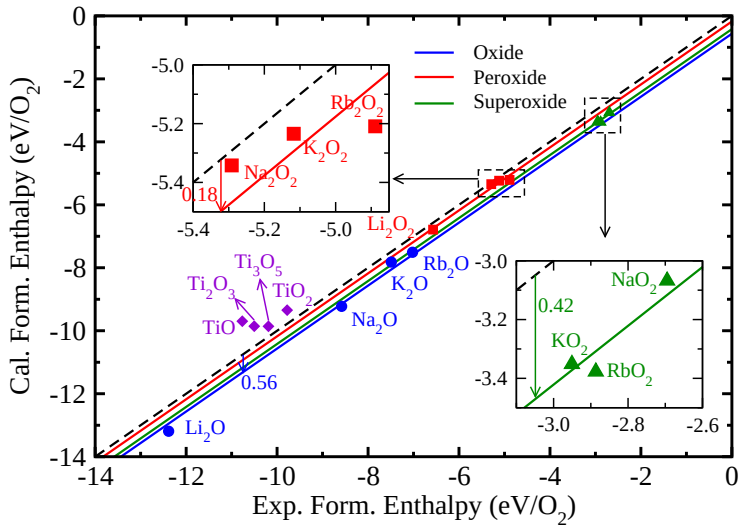

Figure S1. The calculated formation enthalpy versus experimental formation enthalpy for alkali metal oxides and titanium oxides. For alkali metal oxides, systematic differences are found, giving the correction energy for oxide formation energy E_{oxd}^{cor} = 0.42, 0.18, and 0.56 eV per O_2 for superoxide, peroxide and oxide, respectively.

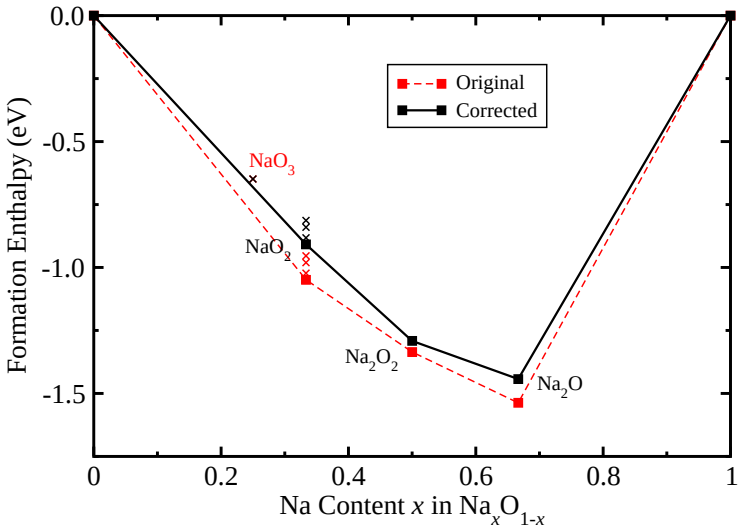

Figure S2. Convex hull plot of formation energies of the binary Na–O system. Red-colored dashed line is for the original formation energies, and black-colored solid line is for the formation energies corrected with $E_{\mathrm{oxd}}^{\mathrm{cor}}$.

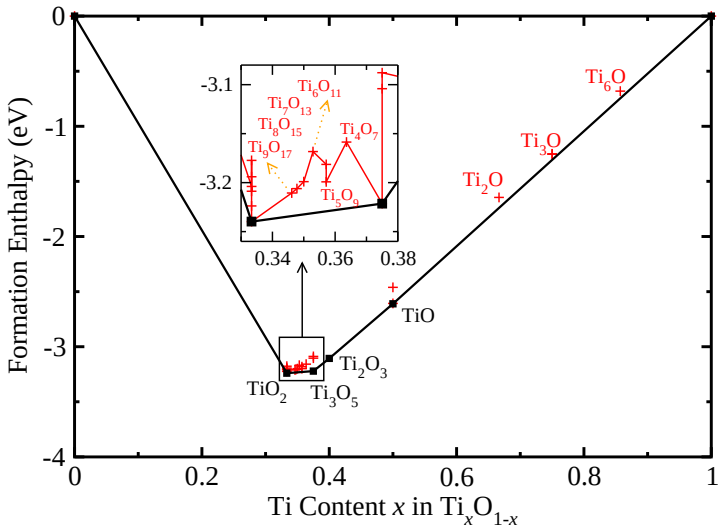

Figure S3. Convex hull plot of formation energies of the binary Ti–O system.

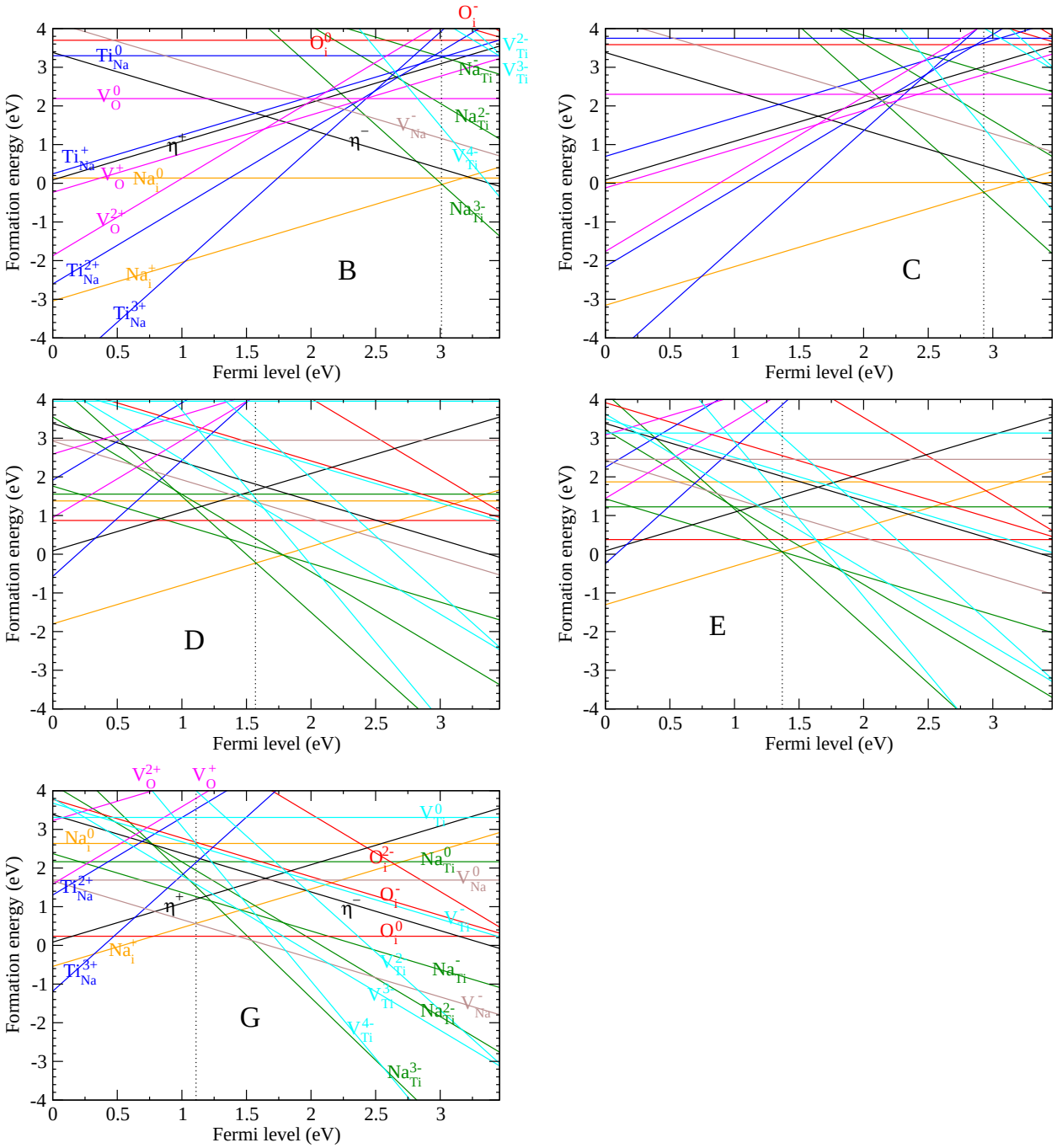

Figure S4. Calculated formation energies of intrinsic point defects with different sets of atomic chemical potentials at the corner points of stable polygon, B, C, D, E, and G.

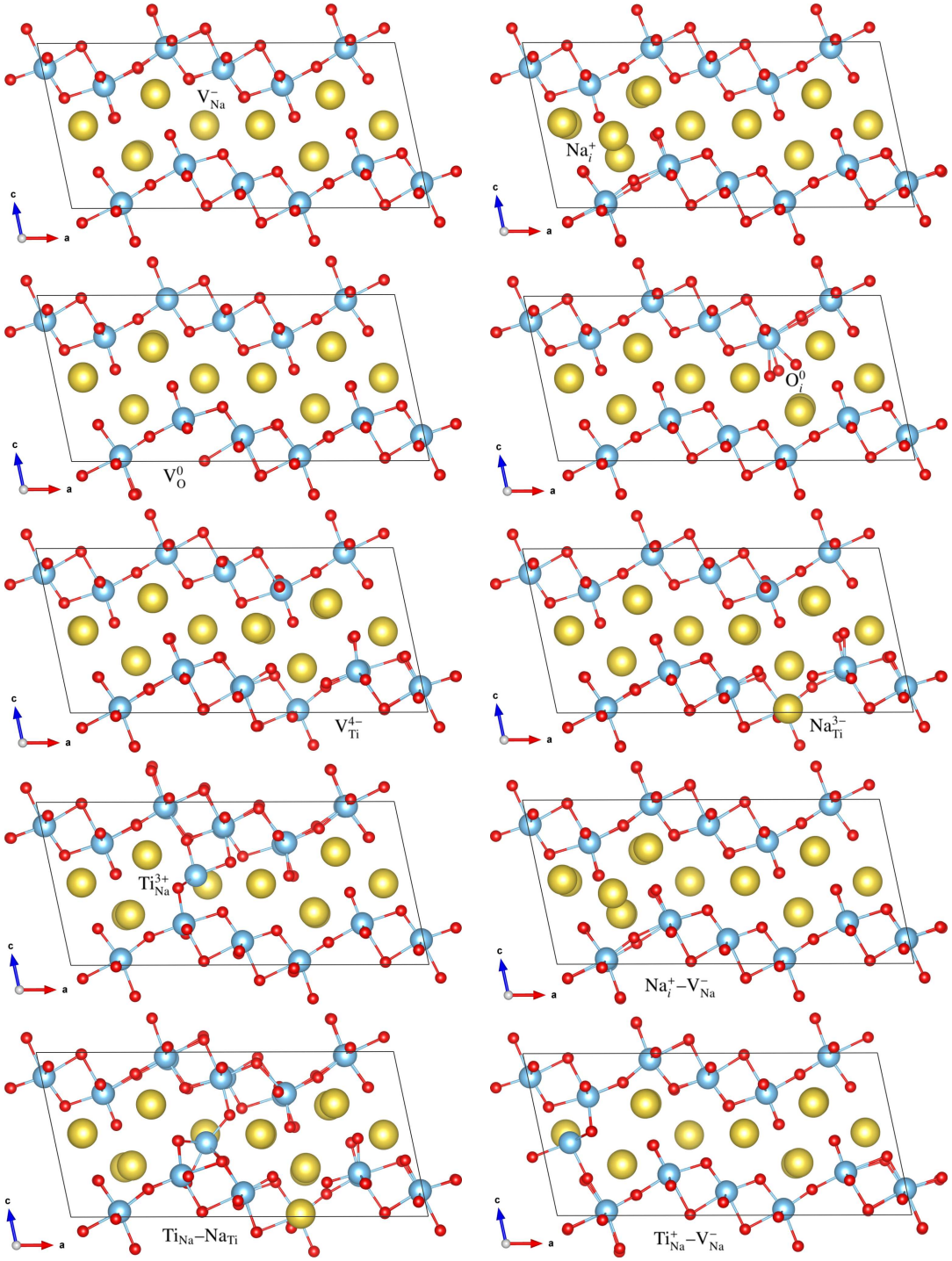

Figure S5. Optimized crystalline structures of defect supercells.

References

[1] H. Pan, X. Lu, X. Yu, Y.-S. Hu, H. Li, X.-Q. Yang, L. Chen, Sodium Storage and Transport Properties in Layered $Na_2Ti_3O_7$ for Room-Temperature Sodium-Ion Batteries, Adv. Energy Mater. **3**, 1186–1194 (2013).

[2] A. A. Araújo-Filho, F. L. R. Silva, A. Righi, M. B. da Silva, B. P. Silva, E. W. S. Caetano, V. N. Freire, Structural, Electronic and Optical Properties of Monoclinic $Na_2Ti_3O_7$ from Density Functional Theory Calculations: a Comparison with XRD and Optical Absorption Measurements, J. Solid State Chem. **250**, 68–74 (2017).

[3] M. W. Chase, Jr., *NIST-JANAF Themochemical Tables*, Fourth Edition (J. Phys. Chem. Ref. Data, Monograph 9, 1998) pp. 11951.

[4] *CRC Handbook of Chemistry and Physics*, Internet Version, D. R. Lide Ed.; CRC Press: http://www.hbcpnetbase.com, Boca Raton, FL (2005).